Research Square

Preprints are preliminary reports that have not undergone peer review.
They should not be considered conclusive, used to inform clinical practice,
or referenced by the media as validated information.

Genomic Characterization and Molecular Evolutionary Analysis of Monkeypox Virus in Qinghai, China, 2025

Bin Guo
Qinghai Provincial Center for Disease Control and Prevention
Qianlan Li
Qinghai Provincial Center for Disease Control and Prevention
Zhijian Tang
Qinghai Provincial Center for Disease Control and Prevention
Mengqi Yin
Qinghai Provincial Center for Disease Control and Prevention
Jinying Qi
Qinghai Provincial Center for Disease Control and Prevention
Youju Lei
Qinghai Provincial Center for Disease Control and Prevention
Jianying Wu
Qinghai Provincial Center for Disease Control and Prevention
Huijun Zhao
Xining Municipal Center for Disease Control and Prevention
Yingxia Chen
Xining Municipal Center for Disease Control and Prevention
Xufang Zhao
Xining Municipal Center for Disease Control and Prevention
Yixin Zhao
Qinghai Provincial Center for Disease Control and Prevention
Xiaotong Wang
Qinghai Provincial Center for Disease Control and Prevention
Xiaoting Zhou
Qinghai Provincial Center for Disease Control and Prevention
Chunxiang Wang
1328647735@qq.com

Qinghai Provincial Center for Disease Control and Prevention

Article

Keywords: Mpox virus, Whole-genome sequencing, Phylodynamic, Micro-evolution, Lineage E.4, Protein stability

Posted Date: November 11th, 2026

DOI: https://doi.org/10.21203/rs.3.rs-11108541/v1

License: This work is licensed under a Creative Commons Attribution 4.0 International License. Read Full License

Additional Declarations: No competing interests reported.

Genomic Characterization and Molecular Evolutionary Analysis of Monkeypox Virus in Qinghai, China, 2025

Bin Guo*[1], Qianlan Li*[1], Zhijian Tang*[1],(these authors contributed equally) Mengqi Yin[1], Jinying Qi[1], Youju Lei[1], Jianying Wu[1], Huijun Zhao[2], Yingxia Chen[2], Xufang Zhao[2], Yixin Zhao[1], Xiaotong Wang[1], Xiaoting Zhou[1], Chunxiang Wang*[1]1328647735@qq.com

[1]Qinghai Provincial Center for Disease Contral and Prevention, Xining, Qinghai, China

[2]Xining Municipal Center for Disease Contral and Prevention, Xining, Qinghai, China

Abstract

Monkeypox virus (MPXV) lineage E.4 has emerged as the predominant strain in Asia, however, genomic data from northwestern China remains scarce. In this study, we performed comprehensive genomic, phylodynamic, and structural analyses of three newly identified MPXV isolates obtained from confirmed cases in Qinghai Province, China, between June and September 2025. Whole-genome sequencing, optimally performed on vesicular fluid owing to peak viral loads—confirmed that all isolates belong to Clade IIb, lineage E.4, and form a tight monophyletic cluster with contemporary strains from Japan. Bayesian phylodynamic reconstruction yielded a mean evolutionary rate of 4.186×10^{-5} substitutions per site per year and revealed a rapid population expansion between June and September 2025, coinciding with the regional rise of the E.4 lineage. Notably, mutational profiling uncovered a distinctive “core conserved, terminal differentiated” pattern. Although all isolates shared 11 signature mutations, substantial sample-specific heterogeneity—including eight unique mutations restricted to a single isolate—strongly suggest multiple independent introductions into Qinghai through a cryptic transmission network, rather than a single localized outbreak. In silico predictions further identified OPG102:T150I and OPG092:E155K as highly deleterious mutations that severely destabilize protein structure ($\Delta\Delta G$ = –0.64 and –0.13 kcal/mol, respectively). We hypothesize that these structural perturbations represent adaptive fitness trade-offs that may prioritize conformational flexibility or immune evasion. Collectively, these findings underscore the critical need for high-resolution genomic surveillance, integrated with structural bioinformatics, to decipher the ongoing microevolution of MPXV.

Keywords: Mpox virus; Whole-genome sequencing; Phylodynamic; Micro-evolution; Lineage E.4; Protein stability.

Introduction

Mpox is a zoonotic disease caused by the monkeypox virus (MPXV), a double-stranded DNA virus belonging to the genus Orthopoxvirus, which also includes the variola, vaccinia, and cowpox viruses [1,2]. Although the clinical manifestations of mpox can be indistinguishable from those of smallpox at certain stages of disease progression, they are generally milder and associated with a lower mortality rate[3]. The incubation period typically ranges from 4 to 14 days, with occasional extensions up to 21 days[3,4]. Disease onset is characterized by a febrile prodrome accompanied by headache, myalgia, back pain, malaise, and diaphoresis. One to three days after fever onset, a rash emerges on the face, oral mucosa, extremities, chest, anogenital region, and conjunctivae[5]. The lesions progress sequentially through macular, papular, vesicular, and pustular stages before crusting over and desquamating, at which point the patient is no longer considered infectious[4,6]. Although recent studies have confirmed the presence of MPXV in male semen [7,8], whether the virus persists in or is transmitted via the female vaginal tract remains under investigation [9,10].

Initially isolated from captive monkeys in a Danish laboratory in 1958—which led to the historical misnomer "monkeypox" [11]—MPXV is now understood to have African rodents,

including squirrels and Gambian pouched rats, as its principal natural reservoirs, rather than non-human primates [12,13]. According to recent historical reviews, the first recorded human case occurred in the Democratic Republic of the Congo (DRC) in 1970[14]. In 2003, the United States experienced a multistate outbreak linked to imported African rodents, marking the first documented mpox outbreak outside the African continent [15]. By late 2024, the World Health Organization (WHO) had received reports of over 130,000 suspected and confirmed mpox cases across more than 130 countries , underscoring the disease's expansive geographic footprint, with the heaviest burdens observed in Africa, Europe, Southeast Asia, and the Americas [16].

Epidemiological data consistently demonstrate a male predominance in mpox cases, primarily driven by transmission networks among men who have sex with men (MSM) [17]. Transmission predominantly requires direct, close interpersonal contact with an infected individual[18,19]. Although respiratory droplets have been implicated as a potential transmission route, current evidence does not support highly efficient airborne dissemination comparable to that of SARS-CoV-2. Furthermore, unlike SARS-CoV-2, MPXV is generally not contagious prior to symptom onset [3]. Consequently, the isolation of symptomatic individuals and rigorous contact tracing remain highly effective public health interventions for interrupting transmission chains. Infection can also occur via other portals of entry, including the oropharynx, nasopharynx, and transdermal routes [3,11].

Genomic sequencing has established that MPXV comprises two major phylogenetic clades—designated Clade I and Clade II—which exhibit distinct epidemiological features and virulence profiles [20]. Clade I is historically associated with significantly higher case fatality rates and greater morbidity. Notably, a rapidly expanding outbreak in the DRC in early 2024 was driven by a novel Clade I variant, designated Clade Ib (first identified in September 2023) [21]. This sublineage exhibits distinct molecular alterations, most notably the deletion of probe and primer target sequences required for established Clade I-specific PCR assays, posing significant new challenges for disease surveillance and diagnostics [21].

In contrast to Clade I, Clade II is historically endemic to West Africa and diverges into two phylogenetically distinct sublineages: IIa and IIb [20]. Sublineage IIa generally induces milder clinical disease and maintains a low case fatality rate. Conversely, sublineage IIb—specifically the B.1 lineage—was the primary driver of the 2022 global mpox pandemic [1,22]. This lineage demonstrated enhanced human-to-human transmissibility, facilitating rapid dissemination into non-endemic regions and establishing sustained transmission within MSM populations. Subsequently, B.1 diversified into multiple descendant lineages[23]. Recent surveillance has documented the emergence of the C.1.1 lineage (a derivative of B.1) across Asia[24,25]. Furthermore, lineages E.1 through E.4, which evolved from C.1.1, have been detected in Europe and, more recently, in Guangdong, China [26]. The identification of lineage E.4 in the three MPXV isolates characterized in the present study strongly suggests that the E lineage is currently the dominant circulating variant in China. However, understanding of population susceptibility to these emerging lineages and the evolutionary determinants driving their spread remains critically limited. This knowledge gap necessitates rigorous molecular epidemiological investigations.

Therefore, in this study, we performed whole-genome sequencing and phylogenetic analysis of three mpox cases identified in Qinghai Province between June and September 2025.Through comparative genomic analyses with global reference sequences, we aim to elucidate the epidemiological characteristics, transmission dynamics, and microevolutionary relationships of

circulating MPXV strains, ultimately providing an evidence base for regional outbreak prevention and public health responses.

Result

Epidemiological Characteristics of MPXV Cases

Between June and September 2025, clinical specimens were collected from three laboratory-confirmed mpox patients in Xining City, Qinghai Province, China. Epidemiological investigations revealed that all three patients were male (median age: 38 years; range: 35–42) with no recent history of international travel. Notably, all patients reported male-to-male sexual contact (MSM) within the 21 days preceding symptom onset, further implicating MSM networks as the primary driver of the regional mpox transmission chain. As detailed in Table 1, diverse clinical specimens were collected based on individual disease progression, including oropharyngeal or nasopharyngeal swabs, vesicular fluid, crusts, and blood. Crucially, vesicular fluid was successfully acquired from all three patients.

Viral Load Assessment via qPCR

Real-time quantitative PCR (qPCR) was performed on all clinical specimens collected from the three mpox patients. As detailed in Table 2, all samples tested positive for MPXV DNA. Notably, vesicular fluid samples consistently yielded the lowest Ct values (range: 18.27–22.93), indicating the highest viral loads among all evaluated specimen types. In contrast, respiratory samples (oropharyngeal and nasopharyngeal swabs) and blood specimens exhibited substantially higher Ct values (range: 30.71–34.73 and 35.39–35.67, respectively), reflecting lower viral shedding in these compartments. Furthermore, the crust specimen from Patient 2025001 yielded a relatively low Ct value (21.20), demonstrating that skin lesions maintain persistently high viral loads even as they crust over. Consequently, these findings clinically validate that vesicular fluid is the optimal specimen type for both primary MPXV diagnostic detection and subsequent whole-genome sequencing.

Whole-Genome Sequencing and Assembly Results

Whole-genome sequencing of the MPXV-positive specimens was successfully performed using the MGI platform. The raw data output averaged approximately 1.7 Gb per sample, and the proportion of high-quality bases (Q30) for each sample exceeded 94%. Reads were mapped against the reference genome (GenBank accession: NC_063383), and consensus sequences were generated utilizing a minimum depth threshold of 10×. As detailed in Table 3, this pipeline yielded three near-complete MPXV genomes with sequence lengths ranging from 197,154 to 197,207 bp, achieving a remarkable genome coverage of 99.97% across all isolates.

Temporal dynamics and evolutionary succession of MPXV lineages

An integrated analysis of lineage assignment, geographic origin, and temporal metadata revealed distinct spatiotemporal distribution patterns and dynamic evolutionary trajectories of MPXV across the Asian region. While high-frequency lineages naturally dominate the visual intensity of the heatmaps (Fig. 1), underlying sequence metadata confirm the concurrent presence of minor, low-frequency variants.

In 2022, the viral population within clade IIb was predominantly characterized by lineage A.2 and its sublineage A.2.1 (Fig. 1b). Lineage A.2.1 showed a marked cluster in India, with sporadic detections in Thailand. Concurrently, lineage B.1 and its sublineages (e.g., B.1.1, B.1.5) were intermittently distributed across Japan, the Philippines, Georgia, and South Korea. This distribution, as reflected by the scattered low-intensity signals in the geographic heatmap, suggests that the early

phase of the epidemic was characterized by the coexistence of multiple lineages with a relatively fragmented regional footprint (Fig. 1a). Furthermore, the detection of the H.1 lineage in South Korea indicates a certain degree of lineage complexity during this initial period.

In 2023, a major epidemiological shift occurred as lineage C.1 rapidly emerged and became the predominant circulating strain (Fig. 1b). It became widely distributed across multiple East and Southeast Asian countries, exhibiting intense clustering particularly in Japan and Indonesia, alongside South Korea and Thailand (Fig. 1a). Notably, the number of sequences from Japan and South Korea increased substantially, indicating robust and sustained transmission networks for this lineage within the region. Concurrently, lineage C.1 diversified into several sublineages (e.g., C.1.1, C.1.3), which were detected in China, Japan, and Thailand, reflecting ongoing genetic differentiation of the virus during regional spread. In addition, lineage H.2 began to emerge in isolated cases in Pakistan and India, suggesting that certain low-frequency lineages managed to persist within the region.

Phylogenetic Characteristics of MPXV Isolates from Qinghai

To elucidate the evolutionary relationships, geographic provenance, and spatiotemporal dynamics of the MPXV isolates, a comprehensive circular phylogenetic tree was constructed using whole-genome sequences. The tree topology integrates multiple concentric colored bands that encode the lineage assignment, country of origin, and sampling timeline (month and year) for each analyzed isolate (**Fig. 2**). The central branching structure depicts the phylogenetic relationships among the genomes, with branch lengths strictly proportional to the genetic distances between samples.

Phylogenetic analysis unambiguously assigned the three isolates from Qinghai Province (MPOX/CHN/Qinghai/2025001–2025003) to Clade IIb, Lineage E.4. Within the broader context of the regional viral population, these three Qinghai genomes form a highly supported, tight monophyletic cluster. They exhibit exceptional genetic homology and occupy immediately adjacent terminal branches on the tree, strongly indicating that they originated from a single, recent introduction event and share a common local transmission chain. Crucially, this Qinghai cluster positions adjacently to a specific subclade comprising MPXV isolates from Japan (the TMIPH series). The marked genetic consistency between the Qinghai and Japanese isolates, characterized by near-zero genetic distances in certain sequence pairs, recapitulates the evolutionary history of the virus and underscores the cross-border transmission heterogeneity driving the current regional outbreak.

Evolutionary dynamics of MPXV clade IIb

Bayesian Skyline Plot (BSP) analysis revealed that the relative effective population size of MPXV remained at a low and stable level from 2020 to early 2022. Following a brief decline in mid-to-late 2022, the population experienced a rapid, exponential increase beginning in 2023, ultimately peaking between late 2023 and early 2024. This trajectory suggests a massive population expansion and intensified transmission during this window. After 2024, the relative effective population size gradually declined and continued this downward trend through 2025, indicating a waning expansion phase and a reduction in transmission scale. Overall, the demographic history illustrates a dynamic process of "low-level maintenance → rapid expansion → gradual decline" for MPXV over the study period (**Fig. 3a**).

The time-scaled phylogenetic tree (**Fig. 3b**) estimated the mean evolutionary rate of MPXV clade IIb at 4.186×10^{-5} substitutions/site/year (ESS = 6157), with a 95% highest posterior density

(HPD) interval of 3.670×10^{-5} to 4.716×10^{-5}. This high ESS value indicates robust MCMC convergence, providing a highly reliable temporal signal for estimating divergence times and the time to the most recent common ancestor (tMRCA).

Molecular clock analysis estimated the tMRCA of the ancestral MPXV clade IIb in Asia to be approximately 2016 (**Fig. 3b**). Subsequently, three major geographic clades diverged. The India-dominant clade emerged with a tMRCA of 2019, suggesting the early establishment of an independent transmission cluster. The Japan/South Korea-dominant clade diverged with a tMRCA of 2021.17, representing the major East Asian lineage. Nested within this lineage, the Indonesia-dominant subclade exhibited a more recent tMRCA of 2022, indicating intense localized expansion. Notably, the three newly characterized Qinghai isolates form a tight cluster within the post-2021 Japan/South Korea-dominant expansion, further corroborating their recent divergence from this established East Asian transmission network.

Collectively, the common ancestor of MPXV clade IIb in Asia dates to approximately 2016, leading to the emergence of multiple region-specific clades between 2019 and 2022. The distinct grouping of sequences from India, Indonesia, and Japan/South Korea strongly suggests that the recent spread of MPXV in Asia is not a product of homogeneous diffusion, but rather driven the parallel evolution and asynchronous expansion of multiple region-associated transmission clusters.

Whole-Genome Genetic Distance and Hierarchical Clustering

Pairwise genetic distances among the sampled isolates were calculated based on whole-genome sequences, followed by hierarchical clustering. A $\log_{10}$transformation was applied to the distance matrix to enhance the resolution of minimal genetic divergence. Contrary to a strict geographic separation, the structured distribution of genetic distances (Fig. 4) reveals a deep evolutionary intermingling between the Chinese and Japanese isolates.

The hierarchical dendrogram demonstrates that the three Qinghai isolates (MPOX/CHN/Qinghai/2025001–2025003) do not form a single, isolated outgroup; rather, they are nested intimately within the genetic diversity of the Japanese TMIPH series. Specifically, within-group comparisons reveal that Qinghai isolates 2025001 and 2025002 share an extremely low genetic distance (approaching zero, indicated by black blocks), suggesting a direct transmission link or an identical recent ancestor. Furthermore, these two genomes cluster tightly with the Japanese isolate TMIPH-0518. Intriguingly, the third Qinghai isolate (2025003) clusters in a distinct sub-branch alongside Japanese isolates TMIPH-0520 and TMIPH-0588, rather than directly with the other Qinghai samples.

Overall, cross-group comparisons showed that the maximum genetic distance across all evaluated genomes remains remarkably low (approximately 10^{-4}), reflecting a very recent common evolutionary background for this regional outbreak. The clear block-like pattern in the heatmap, characterized by interspersed geographic origins, strongly suggests a highly interconnected regional transmission network and raises the possibility of multiple, independent introduction events into Qinghai from the broader East Asian circulating pool.

Mutation Spectrum Analysis of MPXV Isolates from Qinghai

Having established the macro-evolutionary positioning and tight genetic clustering of the Qinghai isolates, we next sought to pinpoint the specific molecular drivers underlying this micro-evolution. A binary presence/absence matrix was constructed to map the distribution of 26 non-synonymous amino acid substitutions across the OPG genes of the three Qinghai isolates (Fig. 5).

To pinpoint the specific molecular drivers underlying this microevolution, we constructed a binary presence/absence matrix mapping the distribution of 26 non-synonymous amino acid substitutions across the OPG genes of the three Qinghai isolates (Fig. 5). In this matrix, red blocks (1.0) indicate the presence of a specific mutation, while blue blocks (0.0) indicate its absence relative to the reference sequence. The distinct mutational profiles highlight a conserved core signature shared by all three isolates, alongside significant sample-specific heterogeneity that distinguishes isolate 2025003 from the 2025001/2025002 cluster.

Furthermore, the mutation spectrum exhibited distinct sample-specific heterogeneity, perfectly corroborating the subtle bifurcations observed in the whole-genome hierarchical clustering (Fig. 4). Specifically, a subset of mutations—OPG102:T150I, OPG112:P70S, OPG114:D82N, OPG122:E26K, and OPG209:T131S—was exclusively shared by isolates 2025001 and 2025002. In stark contrast, a completely divergent set of mutations—OPG015:S3L, OPG015_dup:S3L, OPG043:D136N, OPG043:P139L, OPG087:D39N, OPG088:S28F, OPG122:N133D, OPG144:M40I, and OPG190:E62K—was exclusively detected in isolate 2025003. This pronounced disparity in the terminal mutation spectra strongly suggests that isolate 2025003 has undergone an independent micro-evolutionary trajectory, further supporting the hypothesis of multiple independent introductions into Qinghai rather than a single, homogeneous transmission chain.

Functional Consequence and Thermodynamic Stability Predictions

To evaluate the potential phenotypic impact of the identified non-synonymous mutations, *in silico* functional predictions were performed using PolyPhen-2. While the majority of the mutations scored low—suggesting they are likely benign—a specific subset exhibited high scores indicative of deleterious functional consequences. Notably, OPG102:T150I emerged as one of the highest-scoring alterations (HumDiv: 0.995; HumVar: 0.862), and OPG092:E155K also presented substantial penalty scores (HumDiv: 0.986; HumVar: 0.798), warranting further structural investigation.

To quantitatively assess the structural impact of these critical mutations, thermodynamic stability analyses were performed using DynaMut2. Consistent with the PolyPhen-2 predictions, both candidates were predicted to induce structural destabilization. Specifically, OPG092:E155K exhibited a $\Delta\Delta G$ of -0.13 kcal/mol, indicating a mild reduction in protein stability. More strikingly, OPG102:T150I yielded a highly negative $\Delta\Delta G$ of -0.64 kcal/mol, suggesting a pronounced destabilizing effect on the overall protein architecture.

To elucidate the molecular basis of this thermodynamic destabilization, three-dimensional spatial modeling was conducted for both critical sites (Fig. 6). For OPG092:E155K (Fig. 6a), the drastic non-conservative substitution replaces an acidic glutamic acid (E) with a basic lysine (K). This charge reversal significantly alters the local electrostatic surface potential, and the bulky lysine side chain visibly disrupts the native non-covalent interaction networks within the structural cleft.

Similarly, the structural mapping of the highly destabilizing OPG102:T150I mutation (Fig. 6b) provides clear visual evidence for the calculated thermodynamic penalty. This mutation involves the replacement of a polar threonine (T) with a bulky, highly hydrophobic isoleucine (I). The magnified views demonstrate that the loss of the threonine hydroxyl group abolishes native hydrogen-bonding interactions. Simultaneously, the forced introduction of a hydrophobic isoleucine side chain into this microenvironment likely induces steric hindrance and local

conformational stress, perfectly corroborating the significant drop in folding stability (-0.64 kcal/mol). Together, these dual structural and thermodynamic disruptions make OPG102:T150I and OPG092:E155K the top priority candidate mutations driving the micro-evolutionary adaptation of this local transmission cluster.

Discussion

In this study, we conducted comprehensive genomic analyses of three MPXV isolates (MPOX/CHN/Qinghai/2025001–2025003) collected from laboratory-confirmed mpox cases in Qinghai Province, China, from June to September 2025. Our integrated genomic, phylodynamic, and structural analyses provide critical insights into the lineage patterns, cross-border micro-evolution, and underlying functional adaptations of MPXV in this under-sampled region.

Phylogenetic analysis confirmed that all three Qinghai isolates belong to clade IIb, lineage E.4. They exhibited high genetic homology and formed a tight monophyletic cluster with Japanese TMIPH series isolates within the broader Asian E.4 clade. a placement aligns seamlessly with contemporary genomic surveillance data from other regions[34]. Tracing the evolutionary footprints of MPXV in Asia, a 2024 study identified a distinct clustering of C.1 strains in Northeast Asia in 2023 and documented the subsequent rise of descendant E lineages[24]. Our temporal analysis of lineage succession—from A.2 in 2022, to a brief C.1-dominated phase in 2023, to the expansion of E.4 in 2024–2025—mirrors the evolutionary trajectories reported across East Asia, including Japan, South Korea, and other parts of China[25,26]. For instance, an analysis of the 2023 Shenzhen MPXV outbreak indicated that local viruses were primarily imported, establishing stable transmission chains in the MSM population, with some early samples belonging to the C.1.1 lineage[26,35]. This epidemiological pattern strongly suggests that the E.4 lineage has now achieved regional predominance, likely replacing earlier lineages, and underscores the indispensable utility of continuous genomic surveillance in tracking these shifting dynamics[36,37].

Furthermore, our Bayesian Skyline analysis revealed a sharp increase in the viral population beginning in 2023, peaking from late 2023 to early 2024, before gradually declining through 2025. This rapid expansion phase corresponds directly with the global dissemination of lineage C.1 and its E.4 descendants. Notably, a 2024 study also reported a modest peak in the MPXV population size in late 2023[38]. This temporal correlation between the rise of a highly adapted lineage (C.1/E.4) and a surge in the effective population size provides compelling demographic evidence linking lineage turnover to intensified population-level transmission.

Crucially, despite the overall regional homology and a shared core mutation profile (11 signature mutations including OPG016:R84K, OPG023:R280K, and OPG036:M1I), we detected pronounced microevolutionary bifurcation within the Qinghai samples. The hierarchical mutation distribution revealed that isolate 2025003 harbors eight unique, sample-specific mutations (e.g., OPG015:S3L, OPG043:D136N/P139L, and OPG190:E62K) that clearly differentiate it from the 2025001/2025002 cluster. In contrast to a simple single-introduction model, this distinct "core conservation with terminal diversification" pattern—further corroborated by our whole-genome genetic distance mapping—strongly implicates multiple, independent introduction events into Qinghai from a highly interconnected, cryptic East Asian transmission web[39-41]. These dynamics reveal complex cross-regional and local transmission networks consistent with national observations[42-45], where determining whether MPXV sequences resulted from direct overseas importation or domestic interprovincial spread remains challenging without additional

epidemiological evidence. Given the inherent sampling biases in global databases and the limited sample size of our study, our conclusions represent important preliminary evidence that precisely underscores the urgency of establishing more comprehensive and representative genomic surveillance systems at both global and local levels [42-45].

To investigate the biological consequences of this rapid genetic diversification, in silico functional and thermodynamic analyses were performed. PolyPhen-2 predicted OPG102:T150I and OPG092:E155K as high-impact deleterious mutations, which may truncate the late transcription factor VLTF-1 and consequently affect viral late gene transcription and virion assembly—potentially serving as a key molecular marker for this lineage[34]. These penalty scores are comparable to those reported for critical host-interacting proteins in MPXV, such as OPG147, which enhances immune evasion via TNF-α signaling modulation[46]. Furthermore, DynaMut2 quantitatively predicted severe structural destabilization, particularly for T150I ($\Delta\Delta G_{Stability} = -0.64$ kcal/mol). In the context of viral evolution, such thermodynamic penalties often signify adaptive "fitness trade-offs." We hypothesize that the virus tolerates these local structural destabilizations to gain essential conformational flexibility, thereby facilitating host-receptor binding or driving immune evasion by altering established antigenic epitopes. This phenomenon of rapid, human-host-driven adaptation, potentially accelerated by host APOBEC3 deaminase editing[25,47-49], has been increasingly recognized as a hallmark of the ongoing global MPXV Clade IIb outbreak. However, definitive attribution of the post-2022 mutational excess solely to human APOBEC3-mediated editing remains elusive, as the epidemiological complexity and APOBEC3's potential evolutionary role introduce substantial uncertainty regarding outbreak origins and transmission pathways. Nevertheless, these observations collectively suggest that APOBEC3-mediated evolution represents a persistent process that may emerge as a dominant driver of MPXV adaptation within human populations. These in silico predictions serve as a robust foundational screening, providing a clear rationale for prioritizing *in vitro* functional assays targeting viral replication kinetics and immune escape.

Our study provides vital empirical data optimizing clinical sample collection strategies. Real-time PCR analysis demonstrated that blister fluid consistently yielded the lowest Ct values (range 19.40–22.93), reflecting extremely high viral loads. This finding corroborates large-scale diagnostic reviews showing that lesion swabs maintain a significantly higher positivity rate (91.3%) compared to oropharyngeal swabs (69.5%). Consistent with previous multi-center clinical evaluations, our data reinforces the consensus that skin lesion exudates harbor the most robust viral DNA concentrations, making them the gold standard for reliable molecular diagnostics[50]. For genomic surveillance programs, particularly when facing degraded samples or low viremia, prioritizing blister fluid collection is paramount for maximizing whole-genome sequencing success rates.

In conclusion, this study presents a high-resolution genomic characterization of the emerging MPXV E.4 lineage in Qinghai, China. Our phylodynamic reconstructions validate a regional lineage turnover pattern driving the recent 2023–2024 population expansion. Importantly, by unveiling deep mutational heterogeneity and identifying functionally disruptive, yet selectively tolerated mutations (e.g., T150I and E155K) within a localized cluster, we provide compelling evidence for multiple independent viral introductions and ongoing structural adaptation. These findings underscore the imperative of coupling continuous genomic tracking with structural

bioinformatics to decode the cryptic transmission networks and evolutionary trajectories of MPXV, ultimately informing targeted public health interventions.

Materials and methods

Ethics statement

This study protocol was reviewed and approved by the Ethics Committee of Qinghai Provincial Center for Disease Control and Prevention (Approval No. 2026012). Because this study involved virological surveillance aimed at public health and disease control and used only de-identified residual clinical specimens collected during routine diagnostic and surveillance activities, the requirement for informed consent was waived by the Ethics Committee of Qinghai Provincial Center for Disease Control and Prevention. No identifiable personal information of any patient is included in this manuscript.

Specimen Collection

This study included three laboratory-confirmed mpox cases diagnosed in Xining City, Qinghai Province, between June and September 2025. In accordance with the China Mpox Prevention and Control Plan (2023 Edition) issued by the National Health Commission of China, three types of clinical specimens were collected from the suspected patients: blood samples, skin lesion materials (vesicular fluid and crusts), and nasopharyngeal swabs. All swabs and lesion specimens were immediately placed in viral inactivation transport medium prior to diagnostic testing.

DNA Extraction and qPCR Detection

Inactivated nasopharyngeal swabs, vesicular fluids, crusts, and blood specimens were subjected to MPXV nucleic acid detection[27]. Viral DNA was extracted using a magnetic bead-based extraction kit (Tianlong Technology Co., Ltd., Xi'an, China) according to the manufacturer's protocol and automated extractor instructions. Real-time quantitative PCR (qPCR) amplification was performed on a QuantStudio 5 Real-Time PCR System (Thermo Fisher Scientific) using a commercial MPXV detection kit (Beijing Kinghawk Pharmaceutical Co., Ltd.).

Whole-genome sequencing and assembly

Following the Mpox Prevention and Control Plan (Document No. 16 [2023], National Disease Control and Prevention Administration), whole-genome sequencing (WGS) was performed on MPXV-positive specimens exhibiting a cycle threshold (Ct) value ≤ 32. Target enrichment and purification of viral total DNA were conducted using the ATOPlex MPXV Primer Pool, the ATOPlex DNA Multiplex PCR Amplification Module, and the MGIEasy DNA Purification Beads Kit (all from MGI Tech, China). Subsequently, whole-genome libraries were constructed using the MGIEasy Fast PCR-Free Enzymatic Fragmentation Library Preparation Kit. Sequencing was executed with the PE100 sequencing kit on a DNBSEQ-G99RS high-throughput platform (MGI Tech)[28]. Raw sequencing data underwent rigorous quality control, and genome assembly was performed using the proprietary MPXV whole-genome assembly software provided by MGI Tech.

Genome sequence alignment and preprocessing

Reference MPXV whole-genome sequences with complete temporal and geographic metadata were retrieved from the GISAID database (https://www.gisaid.org). Only high-quality genomes with complete metadata were retained for comparative analysis. The final dataset comprised the three newly sequenced isolates from Qinghai Province (MPOX/CHN/Qinghai/2025001–2025003) alongside representative human MPXV isolates from

across Asia. Sequences exhibiting a high proportion of missing data or marked sequencing anomalies were excluded. Multiple sequence alignment was subsequently performed using MAFFT[29] to ensure nucleotide site consistency across all samples, establishing the foundation for lineage classification, mutational profiling, and genetic distance estimations.

Phylogenetic Analysis

Whole-genome phylogenetic reconstruction was performed under the maximum-likelihood (ML) framework using IQ-TREE[30]. The best-fitting nucleotide substitution model was automatically determined by the built-in ModelFinder. Branch support was robustly assessed using the ultrafast bootstrap approximation with 1,000 replicates. The resulting phylogenetic tree was utilized to elucidate evolutionary relationships and geographic origins of the circulating lineages.

Lineage annotation and mutation site analysis

Lineage annotation was conducted using the Nextclade platform, which systematically assigned each MPXV sequence to its respective clade and lineage. Amino acid substitutions within the OPG genes were extracted from the Nextclade outputs, from which a panel of 26 representative mutation sites was selected for further analysis. To systematically characterize mutation distribution, a binary presence/absence matrix was constructed—where "1" denoted the presence of a specific mutation and "0" indicated its absence. This matrix facilitated subsequent population-level mutational profiling.

Temporal dynamics analysis

To reconstruct the time-scaled phylogeny and population dynamics of MPXV clade IIb, Bayesian evolutionary analysis was conducted using BEAST v1.10.4. The analysis employed the GTR+G+I substitution model, an uncorrelated lognormal relaxed molecular clock, and a Bayesian Skyline coalescent tree prior. The Markov Chain Monte Carlo (MCMC) algorithm was run for 90 million generations, with sampling every 9,000 generations. Convergence was confirmed using Tracer v1.7.2, ensuring that the effective sample size (ESS) for all key parameters exceeded 200. Following a 10% burn-in, a maximum clade credibility (MCC) tree was summarized using TreeAnnotator and visualized in iTOL, with branches annotated by sampling year and geographic origin. Relative effective population sizes over time were inferred from the Bayesian Skyline plot.

Genetic distance calculation

Pairwise genetic distances among the whole-genome sequences were calculated using MEGA7 software based on the Kimura 2-parameter (K2P) model[31], generating a comprehensive genetic distance matrix. To optimally resolve and visualize the extremely low levels of genetic divergence typical among closely related intra-outbreak variants, the distance matrix was subjected to a $\log_{10}$ transformation, thereby enhancing the discriminative power for subtle structural differences.

Functional impact prediction of non-synonymous mutations

The potential functional and structural consequences of non-synonymous amino acid substitutions on MPXV proteins were evaluated using computational modeling. Initially, PolyPhen-2 was utilized to predict the functional impact of identified mutations using both the HumDiv and HumVar models. PolyPhen-2 generates a score ranging from 0 to 1, where values approaching 1 indicate a higher probability of deleterious effects on protein function[32].

For candidate mutations exhibiting high PolyPhen-2 scores, DynaMut2 was subsequently employed to assess their impact on protein structural stability[33]. DynaMut2 calculates the free energy change ($\Delta\Delta G_{\text{Stability}}$) before and after the mutation. A positive value($\Delta\Delta G_{\text{Stability}} > 0$)

suggests a stabilizing effect on the protein structure, whereas a negative value($\Delta\Delta G_{\text{Stability}} < 0$) indicates potential destabilization, expressed in kcal/mol. By integrating functional impairment probabilities from PolyPhen-2 with structural stability predictions from DynaMut2, we systematically screened for candidate mutations with significant potential biological relevance.

Reference

1 Lum, F. M. *et al.* Monkeypox: disease epidemiology, host immunity and clinical interventions. *Nature reviews. Immunology* **22**, 597-613, doi:10.1038/s41577-022-00775-4 (2022).

2 Mitjà, O. *et al.* Monkeypox. *Lancet (London, England)* **401**, 60-74, doi:10.1016/s0140-6736(22)02075-x (2023).

3 Srivastava, S. *et al.* The Global Monkeypox (Mpox) Outbreak: A Comprehensive Review. *Vaccines* **11**, doi:10.3390/vaccines11061093 (2023).

4 Adler, H. *et al.* Clinical features and management of human monkeypox: a retrospective observational study in the UK. *The Lancet. Infectious diseases* **22**, 1153-1162, doi:10.1016/s1473-3099(22)00228-6 (2022).

5 Thornhill, J. P. *et al.* Monkeypox Virus Infection in Humans across 16 Countries - April-June 2022. *The New England journal of medicine* **387**, 679-691, doi:10.1056/NEJMoa2207323 (2022).

6 Tarín-Vicente, E. J. *et al.* Clinical presentation and virological assessment of confirmed human monkeypox virus cases in Spain: a prospective observational cohort study. *Lancet (London, England)* **400**, 661-669, doi:10.1016/s0140-6736(22)01436-2 (2022).

7 Lapa, D. *et al.* Monkeypox virus isolation from a semen sample collected in the early phase of infection in a patient with prolonged seminal viral shedding. *The Lancet. Infectious diseases* **22**, 1267-1269, doi:10.1016/s1473-3099(22)00513-8 (2022).

8 Antinori, A. *et al.* Epidemiological, clinical and virological characteristics of four cases of monkeypox support transmission through sexual contact, Italy, May 2022. *Euro surveillance : bulletin Europeen sur les maladies transmissibles = European communicable disease bulletin* **27**, doi:10.2807/1560-7917.Es.2022.27.22.2200421 (2022).

9 Thornhill, J. P. *et al.* Human monkeypox virus infection in women and non-binary individuals during the 2022 outbreaks: a global case series. *Lancet (London, England)* **400**, 1953-1965, doi:10.1016/s0140-6736(22)02187-0 (2022).

10 Huang, S. T. *et al.* The first imported case of monkeypox in Taiwan. *Journal of the Formosan Medical Association = Taiwan yi zhi* **122**, 73-77, doi:10.1016/j.jfma.2022.08.014 (2023).

11 Titanji, B. K., Tegomoh, B., Nematollahi, S., Konomos, M. & Kulkarni, P. A. Monkeypox: A Contemporary Review for Healthcare Professionals. *Open forum infectious diseases* **9**, ofac310, doi:10.1093/ofid/ofac310 (2022).

12 Harapan, H. *et al.* Monkeypox: A Comprehensive Review. *Viruses* **14**, doi:10.3390/v14102155 (2022).

13 Sadeuh-Mba, S. A. *et al.* Monkeypox virus phylogenetic similarities between a human case detected in Cameroon in 2018 and the 2017-2018 outbreak in Nigeria. *Infection, genetics and evolution : journal of molecular epidemiology and evolutionary genetics in infectious diseases* **69**, 8-11, doi:10.1016/j.meegid.2019.01.006 (2019).

14 Breman, J. G. *et al.* Human monkeypox, 1970-79. *Bulletin of the World Health*

Organization **58**, 165-182 (1980).

15 Bunge, E. M. *et al.* The changing epidemiology of human monkeypox-A potential threat? A systematic review. *PLoS neglected tropical diseases* **16**, e0010141, doi:10.1371/journal.pntd.0010141 (2022).

16 Reardon, S. Mpox is spreading rapidly. Here are the questions researchers are racing to answer. *Nature* **633**, 16-17, doi:10.1038/d41586-024-02793-9 (2024).

17 Philpott, D. *et al.* Epidemiologic and Clinical Characteristics of Monkeypox Cases - United States, May 17-July 22, 2022. *MMWR. Morbidity and mortality weekly report* **71**, 1018-1022, doi:10.15585/mmwr.mm7132e3 (2022).

18 Nolen, L. D. *et al.* Extended Human-to-Human Transmission during a Monkeypox Outbreak in the Democratic Republic of the Congo. *Emerging infectious diseases* **22**, 1014-1021, doi:10.3201/eid2206.150579 (2016).

19 Reardon, S. What does the future look like for monkeypox? *Nature* **610**, 250-252, doi:10.1038/d41586-022-03204-7 (2022).

20 Happi, C. *et al.* Urgent need for a non-discriminatory and non-stigmatizing nomenclature for monkeypox virus. *PLoS biology* **20**, e3001769, doi:10.1371/journal.pbio.3001769 (2022).

21 Vakaniaki, E. H. *et al.* Sustained human outbreak of a new MPXV clade I lineage in eastern Democratic Republic of the Congo. *Nature medicine* **30**, 2791-2795, doi:10.1038/s41591-024-03130-3 (2024).

22 Obermeier, P. E. *et al.* Reemergence of Clade IIb-Associated Mpox, Germany, July-December 2023. *Emerging infectious diseases* **30**, 1416-1419, doi:10.3201/eid3007.240092 (2024).

23 Zhao, H. *et al.* The First Imported Case of Monkeypox in the Mainland of China - Chongqing Municipality, China, September 16, 2022. *China CDC weekly* **4**, 853-854, doi:10.46234/ccdcw2022.175 (2022).

24 Chen, Y. C., Liao, Y. C., Mao, Y. C., Yeh, T. K. & Liu, P. Y. Tracing the footprints of MPXV in Asia: phylogenetic insights and lineage dynamics. *Sexually transmitted infections* **100**, 384-387, doi:10.1136/sextrans-2024-056119 (2024).

25 Zhang, S. *et al.* Evolutionary trajectory and characteristics of Mpox virus in 2023 based on a large-scale genomic surveillance in Shenzhen, China. *Nature communications* **15**, 7452, doi:10.1038/s41467-024-51737-4 (2024).

26 Shi, C. *et al.* Phylogenetic and Molecular Evolutionary Insights into Monkeypox Virus Circulation in Shenzhen, China, 2023-2024. *Viruses* **17**, doi:10.3390/v17091214 (2025).

27 Li, Y., Olson, V. A., Laue, T., Laker, M. T. & Damon, I. K. Detection of monkeypox virus with real-time PCR assays. *Journal of clinical virology : the official publication of the Pan American Society for Clinical Virology* **36**, 194-203, doi:10.1016/j.jcv.2006.03.012 (2006).

28 Wan, J. *et al.* Investigation into the epidemiology, genetic characteristics, and clinical manifestations of the first monkeypox outbreak in Shenzhen, China. *Biosafety and health* **5**, 259-265, doi:10.1016/j.bsheal.2023.08.001 (2023).

29 Katoh, K. & Standley, D. M. MAFFT multiple sequence alignment software version 7: improvements in performance and usability. *Molecular biology and evolution* **30**, 772-780, doi:10.1093/molbev/mst010 (2013).

30 Nguyen, L. T., Schmidt, H. A., von Haeseler, A. & Minh, B. Q. IQ-TREE: a fast and

effective stochastic algorithm for estimating maximum-likelihood phylogenies. *Molecular biology and evolution* **32**, 268-274, doi:10.1093/molbev/msu300 (2015).

31 Kimura, M. A simple method for estimating evolutionary rates of base substitutions through comparative studies of nucleotide sequences. *Journal of molecular evolution* **16**, 111-120, doi:10.1007/bf01731581 (1980).

32 Pan, W. *et al.* The first reported case of monkeypox virus clade Ib infection in china-clinical presentation and epidemiologic implications. *International journal of infectious diseases : IJID : official publication of the International Society for Infectious Diseases* **155**, 107881, doi:10.1016/j.ijid.2025.107881 (2025).

33 Cao, R. *et al.* Genomic Surveillance and Phylogenetic Analysis of Monkeypox Virus Sampled from Clinical Monkeypox Cases and Sewage - Sichuan Province, China, 2023. *China CDC weekly* **7**, 1182-1191, doi:10.46234/ccdcw2025.198 (2025).

34 Zhao, Z. *et al.* Evolutionary and Modification Features of Two Monkeypox Virus Strains: Insights from Integrated Genomic and Epigenomic Analyses. *Viruses* **18**, doi:10.3390/v18020259 (2026).

35 Yu, J. *et al.* Phylogeny and molecular evolution of the first local monkeypox virus cluster in Guangdong Province, China. *Nature communications* **14**, 8241, doi:10.1038/s41467-023-44092-3 (2023).

36 Bhatia, S. *et al.* Lessons from COVID-19 for rescalable data collection. *The Lancet. Infectious diseases* **23**, e383-e388, doi:10.1016/s1473-3099(23)00121-4 (2023).

37 Luna, N. *et al.* Phylogenomic analysis of the monkeypox virus (MPXV) 2022 outbreak: Emergence of a novel viral lineage? *Travel medicine and infectious disease* **49**, 102402, doi:10.1016/j.tmaid.2022.102402 (2022).

38 Kraemer, M. U. G. *et al.* Tracking the 2022 monkeypox outbreak with epidemiological data in real-time. *The Lancet. Infectious diseases* **22**, 941-942, doi:10.1016/s1473-3099(22)00359-0 (2022).

39 Jia, H. *et al.* Genomic and epidemiological perspectives on the first local sporadic cases of Mpox in China. *Emerging microbes & infections* **12**, 2245932, doi:10.1080/22221751.2023.2245932 (2023).

40 Dou, X. *et al.* Clinical, epidemiological, and virological features of Mpox in Beijing, China - May 31-June 21, 2023. *Emerging microbes & infections* **12**, 2254407, doi:10.1080/22221751.2023.2254407 (2023).

41 Zhang, D. *et al.* Genetic Features of 84 Genomes of Monkeypox Virus in Recent Circulation - Beijing Municipality, China, 2023. *China CDC weekly* **5**, 918-921, doi:10.46234/ccdcw2023.173 (2023).

42 Molina, I. S. *et al.* Sub-lineage B.1.6 of hMPXV in a global context: Phylogeny and epidemiology. *Journal of medical virology* **95**, e29056, doi:10.1002/jmv.29056 (2023).

43 Borges, V. *et al.* Viral genetic clustering and transmission dynamics of the 2022 mpox outbreak in Portugal. *Nature medicine* **29**, 2509-2517, doi:10.1038/s41591-023-02542-x (2023).

44 Patiño, L. H. *et al.* Phylogenetic landscape of Monkeypox Virus (MPV) during the early outbreak in New York City, 2022. *Emerging microbes & infections* **12**, e2192830, doi:10.1080/22221751.2023.2192830 (2023).

45 Schuele, L. *et al.* Circulation, viral diversity and genomic rearrangement in mpox virus in

the Netherlands during the 2022 outbreak and beyond. *Journal of medical virology* **96**, e29397, doi:10.1002/jmv.29397 (2024).

46 Yi, X. M. *et al.* The conserved poxvirus membrane entry-fusion apparatus component OPG147 targets MITA/STING for immune evasion. *PLoS pathogens* **21**, e1013198, doi:10.1371/journal.ppat.1013198 (2025).

47 Ulaeto, D. O., Dunning, J. & Carroll, M. W. Evolutionary implications of human transmission of monkeypox: the importance of sequencing multiple lesions. *The Lancet. Microbe* **3**, e639-e640, doi:10.1016/s2666-5247(22)00194-x (2022).

48 O'Toole, Á. *et al.* APOBEC3 deaminase editing in mpox virus as evidence for sustained human transmission since at least 2016. *Science (New York, N.Y.)* **382**, 595-600, doi:10.1126/science.adg8116 (2023).

49 Gigante, C. M. *et al.* Multiple lineages of monkeypox virus detected in the United States, 2021-2022. *Science (New York, N.Y.)* **378**, 560-565, doi:10.1126/science.add4153 (2022).

50 Peiró-Mestres, A. *et al.* Frequent detection of monkeypox virus DNA in saliva, semen, and other clinical samples from 12 patients, Barcelona, Spain, May to June 2022. *Euro surveillance : bulletin Europeen sur les maladies transmissibles European communicable disease bulletin* **27**, doi:10.2807/1560-7917.Es.2022.27.28.2200503 (2022).

Authorship contribution stateement

Bin Guo: Writing-original draft, Conceptualization. Qianlan Li: Writing – review & editing. Zhijian Tang: Funding acquisition. Mengqi Yin: Investigation, Data curation. Jinyin Qi: Investigation, Data curation. Youju Lei: Investigation, Data curation. Jianyin Wu: Investigation, Data curation. Huijun Zhao: Investigation, Data curation. Yinxia Chen: Investigation, Data curation. Xufang Zhao: Investigation, Data curation. Yixin Zhao: Investigation, Data curation. Xiaotong Wang: Investigation, Data curation. Xiaoting Zhou: Investigation, Data curation. Chunxian Wang: Funding acquisition, Supervision, Project administration.

Funding

This work was supported by the National Disease Control and Prevention Administration (Public Health Talent Training Support Project, 2024; Chunxiang Wang) and the Qinghai Provincial Government ("Kunlun Talents·High-level Health Talent"Program, 2024; Zhijian Tang).

Date availablility

The three complete genome sequences of Monkeypox virus generated in this study have been deposited in GenBase of the China National Center for Bioinformation (CNCB), Beijing Institute of Genomics, Chinese Academy of Sciences (https://ngdc.cncb.ac.cn/genbase). The accession numbers are C_AA503606.1, C_AA503607.1 and C_AA503608.1, corresponding to isolates MPOX/CHN/Qinghai/2025001, 2025002 and 2025003, respectively.

Declaration of competing interest

The auther declare no conflicts of interest.

Table 1. Demographic and clinical characteristics of the three mpox cases in Qinghai Province, China (2025)

Patient ID	Sex	Age	Location	Date of Onset	Date Of Presentation	Date Of Sampling	Specimen Types
2025001	Male	42	Xining	Jun 24, 2025	Jun 24, 2025	Jun 24, 2025	Oropharyngeal Swab Vesicular fluid

2025002	Male	35	Xining	Jun 17, 2025	Jun 26, 2025	Jul 02, 2025	Crusts Blood Nasopharyngeal Vesicular fluid
2025003	Male	38	Xining	Aug 22, 2025	Aug 26, 2025	Aug 27, 2025	Oropharyngeal Swab Vesicular fluid Blood

Note: Patient IDs (e.g., 2025001) represent the abbreviated forms of the full viral isolate designations (e.g., MPOX/CHN/Qinghai/2025001) used throughout the subsequent nucleic acid and genomic analyses. "Date of Onset" refers to the initial appearance of clinical symptoms. "Date of Presentation" denotes the day the patient first sought medical care. Specimen types varied based on the clinical manifestations present at the time of sampling. All patients were laboratory-confirmed via MPXV-specific qPCR.

Table 2. qPCR viral load detection results of patient specimens

Patient ID	Sample Type	Ct value	Interpretation
2025001	Oropharyngeal Swab	31.80	Positive
	Vesicular fluid	19.40	Positive
	Crust	21.20	Positive
	Blood	35.39	Positive
2025002	Nasopharyngeal	30.71	Positive
	Vesicular fluid	22.93	Positive
2025003	Oropharyngeal Swab	34.73	Positive
	Blood	35.67	Positive
	Vesicular fluid	18.27	Positive

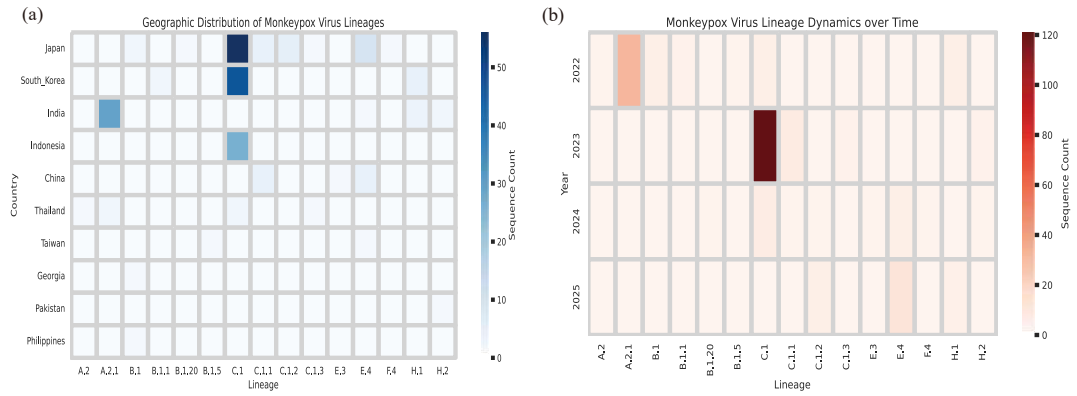
Note: Ct, cycle threshold. According to the diagnostic kit's protocol, a positive detection is defined as a Ct value < 38. A Ct value ≥ 40 is interpreted as negative. A Ct value ranging from 38 to less than 40 falls within the "grey zone" (equivocal/indeterminate), which requires sample re-extraction and retesting for confirmation. Specimens not listed were not collected from the corresponding patient.

Table 3. Summary of MPXV whole-genome sequencing and assembly metrics

Sample ID	Raw-read	Raw-bases(bp)	Assembly-length	(bp) Q30	10x	Coverage
2025001	13,577,305	1,363,124,300	197199	95.93%	197199	99.97%
2025002	20,729,662	2,079,440,100	197207	96.74%	197207	99.97%
2025003	16,418,147	1,657,311,200	197154	94.66%	197154	99.97%

Note: Reference genome used for mapping and coverage calculation was NC_063383. Genome coverage represents the percentage of the reference genome covered by at least 10× sequencing depth.

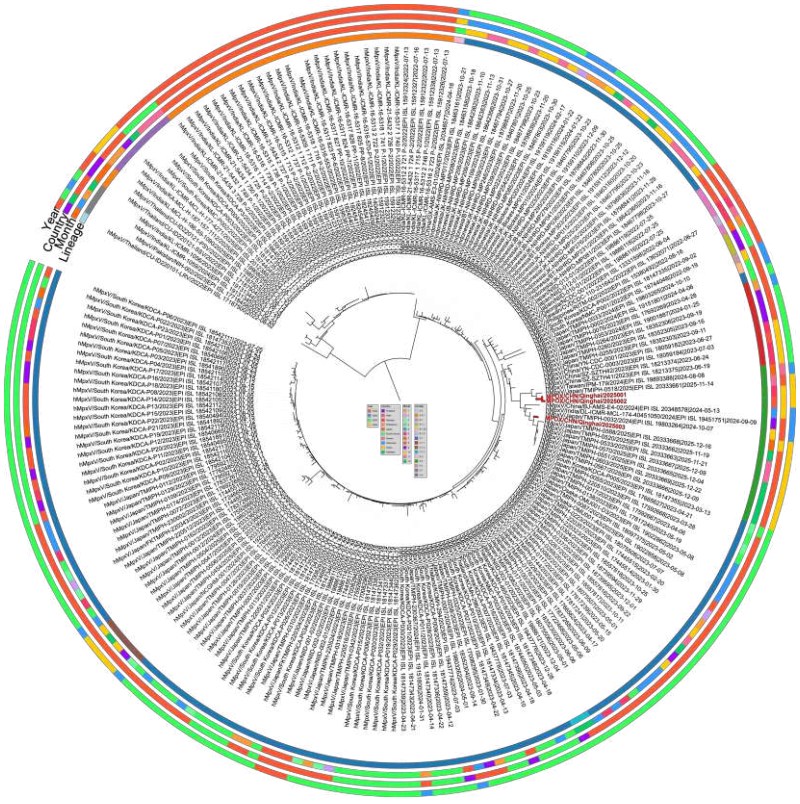
Figure 1. Spatiotemporal distribution and evolutionary succession of MPXV lineages.



(a) Geographic distribution heatmap. The heatmap illustrates the geographic provenance and relative abundance of each lineage across Asia. Color intensity corresponds to the sequence count. Lineage A.2.1 clusters predominantly in India; C.1 exhibits widespread distribution and the highest sequence counts across East and Southeast Asia; and E.4 demonstrates prominent expansion primarily in China and Japan, with sporadic detections in India and Taiwan, China. (b) Temporal dynamics heatmap. The heatmap depicts lineage prevalence and evolutionary succession from 2022 to 2025. Key epidemiological transitions include the scattered coexistence of multiple lineages in 2022, the massive regional expansion of C.1 in 2023 (indicated by the highest sequence count intensity), and the gradual emergence and major presence of E.4 during 2024–2025.

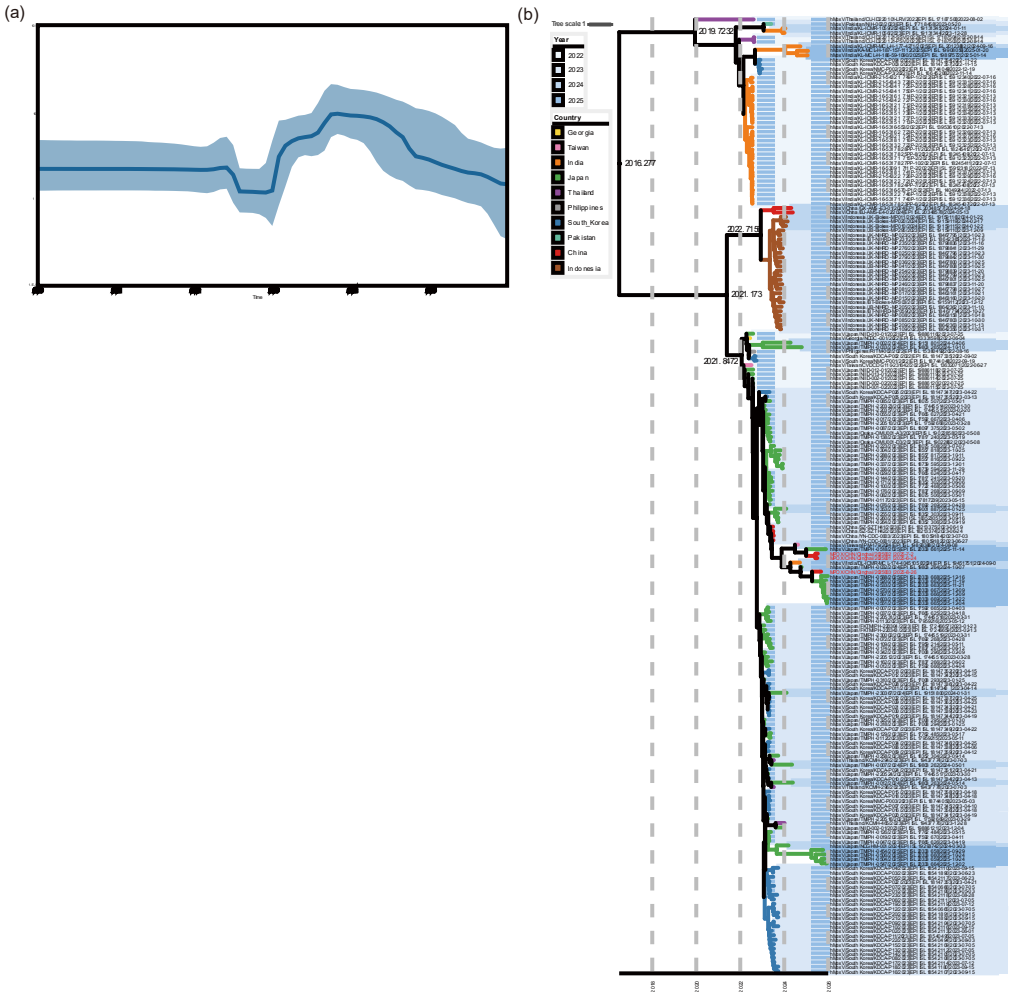
Note: Low-frequency lineages or sporadic regional detections may appear as low-intensity signals due to the linear color scale but are confirmed by underlying sequence metadata.

Figure 2. Circular phylogenetic tree of MPXV genomes.



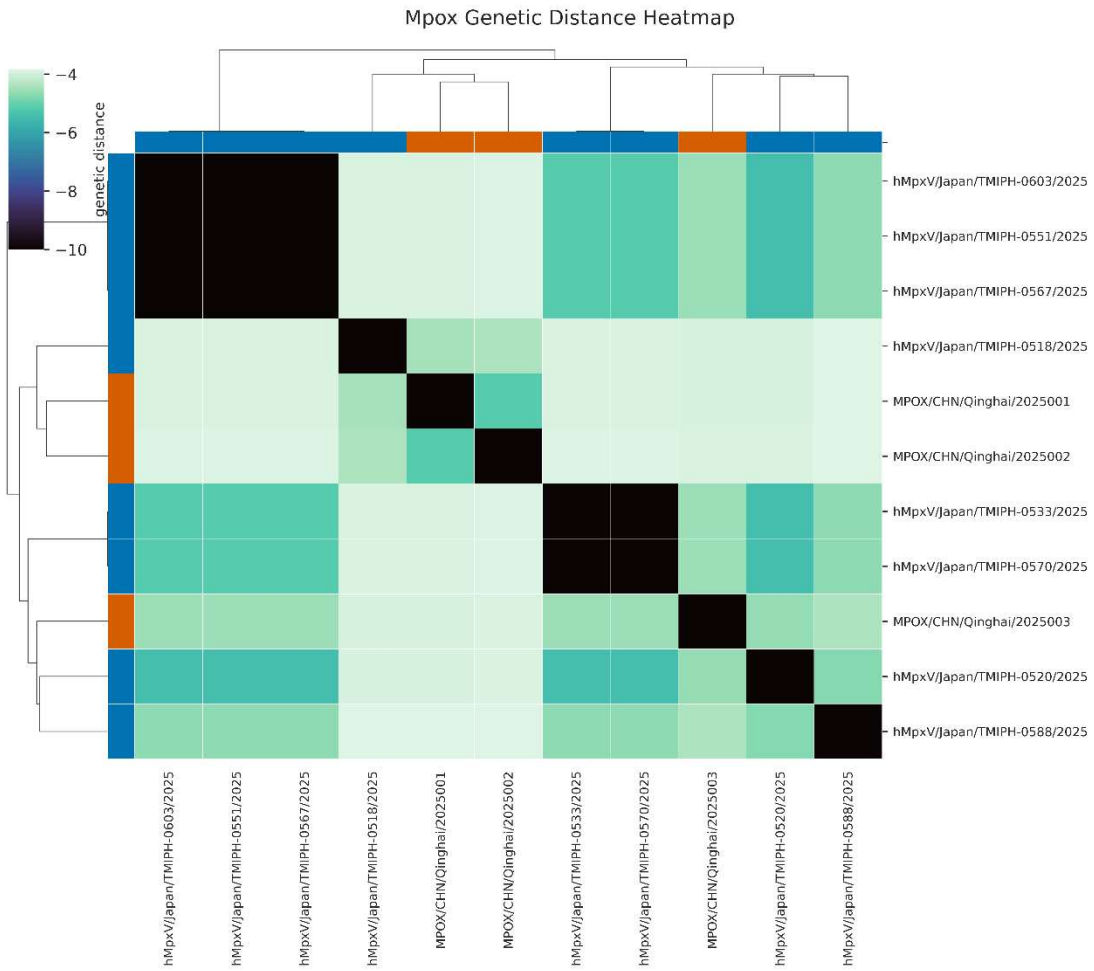
The dendrogram illustrates the genetic relationships among the three Qinghai isolates (highlighted with red text) and other representative regional sequences. Concentric colored rings from the inside out denote lineage assignment, country of origin, and sampling timeline (month and year). The close phylogenetic clustering of the Qinghai isolates with the Japanese TMIPH series within Lineage E.4 highlights their shared evolutionary trajectory.

Figure 3. Evolutionary dynamics and time-scaled phylogenetics of MPXV clade IIb.



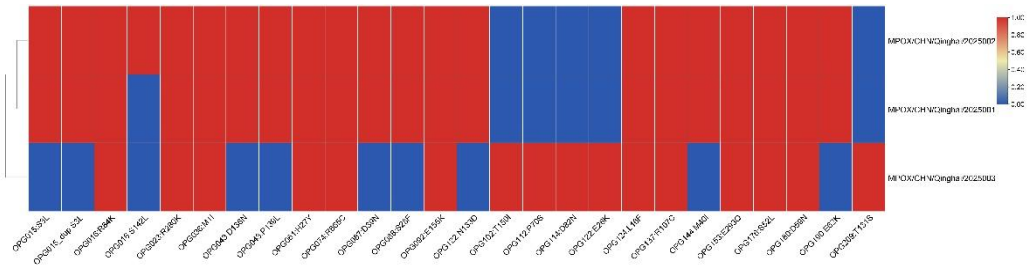
(a) Bayesian Skyline Plot (BSP) depicting the demographic history of the virus. The solid blue line represents the median estimate of the relative effective population size over time, while the blue-shaded area indicates the 95% highest posterior density (HPD) interval. **(b) Maximum clade credibility (MCC) time-scaled phylogenetic tree.** Branch colors indicate the geographic origin of the sequences (e.g., orange for India, brown for Indonesia, green for Japan, and blue for South Korea). The alternating light-blue and white background shading delineates the sampling timeline across consecutive years (2022–2025). The three Qinghai isolates sequenced in this study are explicitly highlighted in red text. Numerical node labels indicate the estimated time to the most recent common ancestor (tMRCA) in years.

Figure 4. Heatmap and hierarchical clustering of whole-genome pairwise genetic distances among MPXV isolates.



The distance matrix was $\log_{10}$transformed to visualize minimal divergence. The color gradient ranges from light mint green (higher genetic distance, approximately10^{-4}) to black (near-zero genetic distance, representing identity or extremely high homology). Top and left annotations indicate geographic origin: orange blocks represent the three isolates from Qinghai, China; blue blocks represent isolates from Japan (TMIPH series). The hierarchical dendrograms illustrate that the Qinghai isolates do not form an isolated clade but are phylogenetically interspersed within the Japanese transmission network, highlighting complex cross-border epidemiological links.

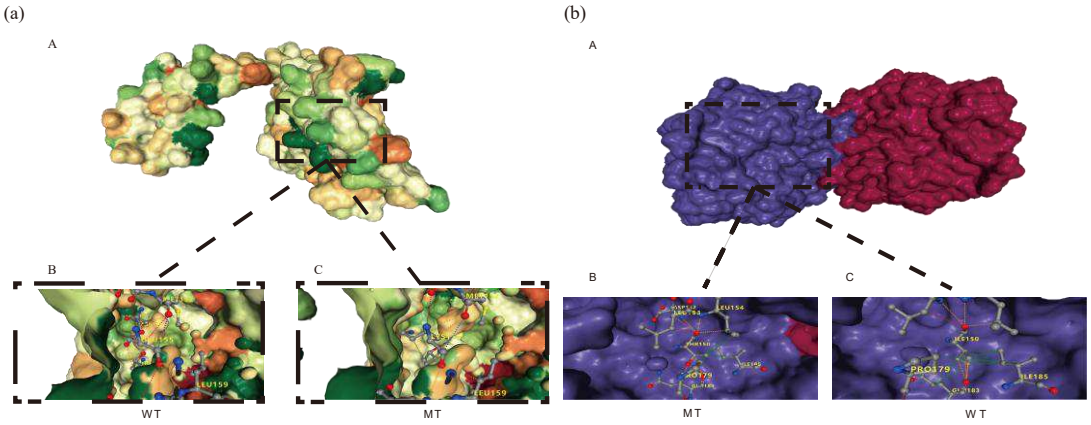
Figure 5. Distribution of the non-synonymous mutation spectra across the three MPXV isolates from Qinghai, China.



The heatmap displays a binary presence/absence matrix of 26 amino acid substitutions located within the OPG genes. Red blocks (1.0) indicate the presence of a specific mutation, while blue blocks (0.0) indicate its absence relative to the reference sequence. The distinct mutational profiles

highlight a conserved core signature shared by all three isolates, alongside significant sample-specific heterogeneity separating isolate 2025003 from the 2025001/2025002 cluster.

Figure 6. Structural and thermodynamic consequences of critical non-synonymous mutations.



(a) 3D spatial modeling of the OPG092:E155K mutation. The magnified insets contrast the wild-type and mutant interaction networks, illustrating how the E-to-K charge reversal disrupts local electrostatic integrity. **(b)** 3D spatial modeling of the OPG102:T150I mutation. The substitution of a polar threonine with a bulky, hydrophobic isoleucine disrupts native hydrogen bonding and induces steric stress, correlating directly with the calculated destabilization penalty ($\Delta\Delta G = -0.64$ kcal/mol).